Activation Temperature and Particle Size of Palm Kernel Shell *vs.* the Surface Properties of Activated Carbon

Chuan Li Lee,[a] Kit Ling Chin,[a,]* Paik San H'ng,[a,b,]* Mohd Sahfani Hafizuddin,[a] and Pui San Khoo [c]

Granular activated carbon (GAC) and powdered activated carbon (PAC) are the two most common forms of activated carbon with varying particle size range. The goal of this study was to analyze the key factors (particle size and activation temperature) affecting the surface characteristics of GAC and PAC derived from palm kernel shell (PKS). The surface morphology suggested that the pore network in PKS-PAC is more developed than that in PKS-GAC owing to the presence of a micropore structure when prepared at lower activation temperatures. This study also demonstrated that activation performed on different PKS particle size range influenced the mesopore domain of the activated carbon produced. The PKS-GAC was found to have more mesopores than PKS-PAC, which made it more reliable for dye adsorption in water treatment. Overall, this study demonstrated that applying different particle size range of PKS during the activation process can have a significant influence on the surface characteristics, thus having a direct impact on the application of activated carbon. An accurate particle size range will ensure that the most cost-effective activated carbon is selected to achieve the desired performance objectives.

Contact information: a: Institute of Tropical Forestry and Forest Products, Universiti Putra Malaysia, 43400 UPM Serdang, Selangor, Malaysia; b: Faculty of Forestry and Environmental, Universiti Putra Malaysia, 43400 UPM Serdang, Selangor, Malaysia; c: Centre for Advanced Composite Materials, Universiti Teknologi Malaysia, 81310 Johor Bahru, Johor, Malaysia;
* Corresponding authors: c_kitling@upm.edu.my; ngpaiksan@upm.edu,my

INTRODUCTION

Green product development has emerged as a global phenomenon, but it has gained attention due to its numerous benefits, including change mitigation, improved energy security, and rural development (Aktar *et al*. 2021). It is undeniable that biomass products can boost Malaysia's sustainable production sector in the future. Malaysia's solid waste production is currently estimated at 33,130 tonnes per day, with a target of 49,670 tonnes per day by 2030 (Bashir *et al*. 2020; Rashidi and Yusup 2021). The palm oil industry generates over 80 MT of solid biomass, with only 10% of oil palm biomass used in the wood and bioenergy industries in 2015 (Demiral *et al*. 2021). Oil palm biomass is used as a source of energy, burned in the field, as mulching material, or spilled into the environment in an uncontrolled manner. The practise of burning biomass causes substantial air pollution and raises public health concerns, while inappropriate biomass waste disposal produces greenhouse gases such as carbon dioxide, nitrous oxide, and methane (Oguntoke *et al*.

2019; Chin *et al*. 2020; Amoatey *et al*. 2021). Thus, reliable waste management is critical to avoid the underutilization of oil palm biomass and to ensure health security, job opportunities for youth, and waste conversion to value-added products.

Bio-carbon has emerged as a hot topic due to the various types of naturally inherited morphology and low-cost fabrication techniques. The use of biomass wastes as starting materials has sparked intense research interest due to their physiochemical stability, light weight, low cost, and environmental friendliness (Aslam *et al*. 2021). Oil palm biomass is an efficient source of carbon for conversion to high-value products especially palm kernel shells (PKS) as activated carbon precursors (Norrrahim *et al*. 2022; Sarwer *et al*. 2022). The high carbon percentage in PKS is promising for the production of activated carbon (AC), as it contributes to a high product yield. In addition, the high strength and hardness of PKS allows it to withstand harsh treatment conditions during the conversion process (Arami-Niya *et al*. 2012; Hidayu and Muda 2016; Joseph *et al*. 2009).

A variety of factors influence the effectiveness of AC for adsorption of pollutants. These factors include the presence of natural organic matter in the raw water, as well as the properties of AC such as pore structure, surface area, raw material, bulk density, and particle size (Bertone *et al*. 2018). Generally, AC is available in two forms: granular activated carbons (GAC) and powdered activated carbons (PAC). GAC has a particle size range of 0.4 to 1.2 mm, whereas PAC has a particle size range of 5 to 50 µm (Philibert *et al*. 2020; Vu *et al*. 2014). To achieve a high adsorption capacity, AC needs a large internal surface area and a well-developed pore structure. In most cases, the majority of the internal surface area is contributed by micropores. Macro and mesopores provide entry to the carbon particle and are essential for kinetics (Olajide 2019; Mendes *et al*. 2015). Given that the particle size ranges of GAC and PAC differ noticeably, the question posed here is whether there is any potential impact of particle size range on performance and application of AC.

The need for precise particle size control is critical as AC applications grow. To ensure optimal performance and to maximize the energy potential, it is essential to select the appropriate type and particle size range. There should be an extensive discussion of the surface characteristic for both ACs made from PKS. Thus, the effect of particle size on surface characteristics of the AC produced from PKS must be thoroughly investigated. A numerical model on the effects of varying AC particle size range on the adsorption properties will help to interpret the results. In addition, the present work investigated the surface characteristics of PKS-GAC and PKS-PAC at various activation temperatures to determine how the process affects the performance of AC.

EXPERIMENTAL

Material

PKS was acquired at the Seri Ulu Langat Palm Oil Mill in Dengkil, Selangor. The sample was thoroughly cleaned and dried at 105 °C for 48 h. The PKS sieving process was carried out using an oscillating screen method to determine the particle size range of GAC and PAC, which are 2 to 5 mm (granular size) and 50 to 85 µm (powdered size), respectively. The particle size range was determined using a vibrating screen method, which provides a measurement of particle width. The sieving time was 20 min, and the amplitude was 10 mm/g. The samples that were retained in the sieve were then collected and stored at 53 ± 2% RH and 24 ± 2 °C.

Methods

Chemical pretreatment

A specified mass of the dried PKS was impregnated with 30% phosphoric acid (H_3PO_4) with an impregnation mass ratio of 1:1 at 80 °C for 2 h. The total mass of the PKS was 500 g, and 500 mL of H_3PO_4 was used in the impregnation process. To remove the excess H_3PO_4, the pretreated particles were filtered and washed with distilled water until the pH reached the specified values (pH 6 to 8) after the pretreatment process. Once the chemical solution was removed, the sample was washed with ambient temperature distilled water (25 to 28 °C) using a solid: liquid ratio of 1:100 (w/v). The H_3PO_4 pretreated samples were filtrated and dried at 105 °C for 48 h prior to the physical activation. The dried pretreated samples were placed in the tube furnace for 3 h to go through the physical activation process at 800, 900, and 1000 °C. PKS-derived ACs (PKS-GAC and PKS-PAC) were stored in desiccators for further evaluation. Each of the 6 treatments (2 particle size range x 3 activation temperatures) was replicated 5 times.

Evaluation

The characteristics of AC included the physiochemical properties such as ash content and mass yield, adsorption properties (iodine and methylene blue), and surface properties. The surface area, surface morphology, and surface analysis were examined as previously described (Lee *et al*. 2017, 2018; Sahfani *et al*. 2021). The BET surface area was determined using a Brunauer-Emmett-Teller analyzer, and the surface functional groups of the samples were analysed using a Fourier Transform Infrared spectroscopy (FTIR) (Perkin Elmer Spectrum 100-IR, Tokyo, Japan). The dry samples were crushed into powder form and were inserted into the FTIR chamber. A Perkin Elmer Spectrum 100 IR spectrometer equipped with an attenuated total reflection (ATR) diamond accessory was employed for collecting the FTIR-ATR spectra of the sample. FTIR-ATR spectra were recorded at wavelengths from 650 to 4000 cm^{-1} with 4 cm^{-1} resolution; for each specimen, 4 scans were collected. In order to analyse the morphology of the AC, the sample prepared at the optimum condition was examined using a Scanning Electron Microscope (SEM). The sample was prepared with the required testing specifications in accordance with the relevant standards, as follows: ash content according to TAPPI T211 om-85 (1992); methylene blue adsorption according to JIS K 1470-1991 (1992); and iodine adsorption according to ASTM D4607-94 (2006). The mass yield of AC was calculated by Eq. 1.

$$\text{Mass yield (\%)} = \frac{\text{Activated carbon(dry),g}}{\text{Precursor (dry),g}} \text{X } 100 \qquad (1)$$

Statistical analysis

The physiochemical and adsorption properties data of the ACs were evaluated for analysis of variance (ANOVA) at a 95% confidence level ($p \leq 0.05$) using the statistical package SPSS for Windows, version 16.0 (SPSS, Chicago, IL, USA). The Tukey-Kramer multiple comparisons test was used to examine the differences between the treatment effects when significance was discovered. In cases where the p-value was greater than 0.05 at the 95% confidence level, the effects were deemed not statistically significant.

RESULTS AND DISCUSSION

Physiochemical and Adsorption Properties of the Activated Carbon

Table 1 summarizes the physiochemical and adsorption properties of PKS-GAC and PKS-PAC. The ANOVA analysis revealed significant effects ($p<0.01$) for the particle size range of AC, physical temperature, and the interaction for the two factors.

According to Table 1, the mass yield of ACs produced was inversely proportional to activation temperature, with a lower mass yield obtained at higher activation temperatures. Both ACs exhibited the most significant mass loss at a temperature of 1000 °C. As stated by Sahfani *et al*. (2021), more volatile matter is released when carbon is activated at a higher temperature, which decreases the yield. Aside from mass yield, ash content percentage compositions were also investigated due to their determinant importance in the selection of the prospective AC's application. The ash content in the PKS-GAC and PKS-PAC increased from 16.7 to 25.6% and 9.8 to 23.0%, respectively, when the temperature was raised from 800 to 1000 °C. The rise in ash content is caused by the gradual concentration of minerals and the destructive volatilization of lignocellulosic materials when temperatures rise (Sahfani *et al*. 2021).

Table 1. Properties of the PKS-GAC and PKS-PAC

Particle Size Range	Temperature (°C)	Chemical Properties		Adsorption Properties	
		Yield (%)	Ash (%)	Methylene Blue Adsorption (mg/g)	Iodine Adsorption (mg/g)
PKS-GAC (2 to 5 mm)	800	38.38[a]	16.68[b]	234.03[f]	543.26[c]
	900	33.21[d]	18.56[c]	397.57[b]	529.30[d]
	1000	30.38[e]	25.61[e]	425.00[a]	350.58[e]
PKS-PAC (50 to 85 µm)	800	36.42[b]	12.28[a]	243.26[e]	762.00[a]
	900	34.92[e]	16.32[b]	256.33[d]	616.80[b]
	1000	27.27[f]	23.49[d]	376.81[c]	322.66[f]
p-value		<0.001	<0.001	<0.001	<0.001

Note: According to Tukey's multiple comparisons test, different letters (a', b', c', d', e' and f') in the same column indicate statistically significant difference at $p < 0.05$.

The performance of ACs may be expressed in terms of yield and adsorption properties, including adsorption of iodine and methylene blue (Chin *et al*. 2020). Iodine adsorption was used to estimate the surface area of an absorbent as well as to provide a measure of the micropores (Lee *et al*. 2018). Furthermore, when the activation temperature was raised from 900 to 1000 °C (refer to Table 1), the iodine adsorption for both ACs declined significantly. An increase in activation temperature from 800 to 1000 °C caused 58% and 36% reduction of iodine adsorption value for PKS-PAC and PKS-GAC, respectively. This result may be due to the filling of micropores with ash products. This interpretation is supported by their negative correlation; high ash content in AC resulted in low adsorption (Hassan *et al*. 2021). It is proposed that the higher activation temperature limited the accessible pathways in the AC.

Adsorption capability also takes into account the adsorbate's accessibility to the AC's internal surfaces, which is determined by the adsorbate molecule size and pore measurements (Borghei *et al*. 2021). According to Samal (2014), methylene blue number is a measure of the mesopore content of the AC. As shown in Table 1, the PKS-GAC had higher methylene blue adsorption than PKS-PAC, indicating that it had more mesopores. Mesopores can easily provide accessible space for faster molecular diffusion, which can

absorb a wider range of molecules (Gualtieri 2021). Hence, PKS-GAC with a relatively high proportion of mesopore volume is highly demanded for both low mass transfer resistance in pores (fast kinetics) and a high equilibrium adsorption capacity of relatively large dye molecules in the textile industry. This study discovered that particle size range had a significant impact on pore distribution, which had a direct impact on the feasibility of AC for various functions. The mesoporous material, PKS-GAC was judged to be much more suitable and feasible for a wider range of applications. Mesopores can serve as a fast electrolyte transfer route in the electrode, whereas the presence of micropores results in a large surface area for ion adsorption (Borghei *et al.* 2021). Furthermore, mesoporous material is more advantageous for monolith use because methane gas (CH_4) adsorption is less sensitive to micropores. This is most likely due to diffusive limitations in smaller pores in the high-pressure region (Borghei *et al.* 2021).

Surface Characteristic of Activated Carbon

Figures 1 and 2 depict the AC surface area and pore structure, respectively. PKS-PAC attained the highest BET specific surface area of 958 m^2/g at an activation temperature of 800 °C. Low activation temperatures were favoured in this study. The average pore width is controlled by the etching temperature. High temperatures increased the average pore width of AC from 1.9 nm to 26.0 nm and 9.1 nm to 16.3 nm for PKS-PAC and PKS-GAC, respectively. The porosity ratio result demonstrated that the physical rupture of the micropores occurred with high temperature.
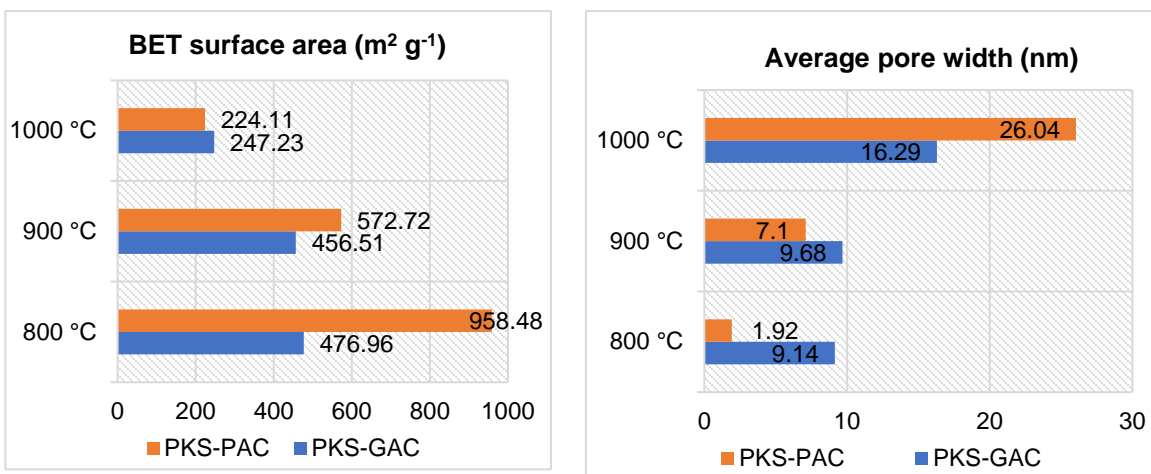
Fig. 1. (a) BET surface area and **(b)** average pore width of PKS-GAC and PKS-PAC
Note: The particle size range of GAC and PAC are 2 to 5 mm (granular size) and 50 to 85 µm (powdered size), respectively.

According to the porosity ratio (Fig. 2(b)), the microporosity region for both ACs was absent at the 1000 °C activation temperature. In contrast, the surface area of the ACs produced at low temperatures was primarily attributable to the micropores. The micropore volume of PKS-PAC prepared with 800 °C was threefold greater than that of PKS-PAC prepared with 1000 °C. This was attributed to the excessive ablation of the carbon structure at high activation temperatures, which causes a fraction of the micropore structure to collapse. Furthermore, the gasification of some of the unstable carbon on the pore wall structure can facilitate the connection of adjacent micropores to synthesise mesopores or macropores. Whilst the rate of micropore destruction exceeds the rate of development, the

percentage of micropores may drop significantly (Zhang *et al*. 2021). Henceforth, the micropore volume decreased dramatically at high temperatures. Upon closer observation, the particle size range was discovered to play a key role in the pore diameters of AC. Even at low temperatures, the average pore width of PKS-GAC was nearly 9 times larger than that of PKS-PAC (Fig. 1(b)).
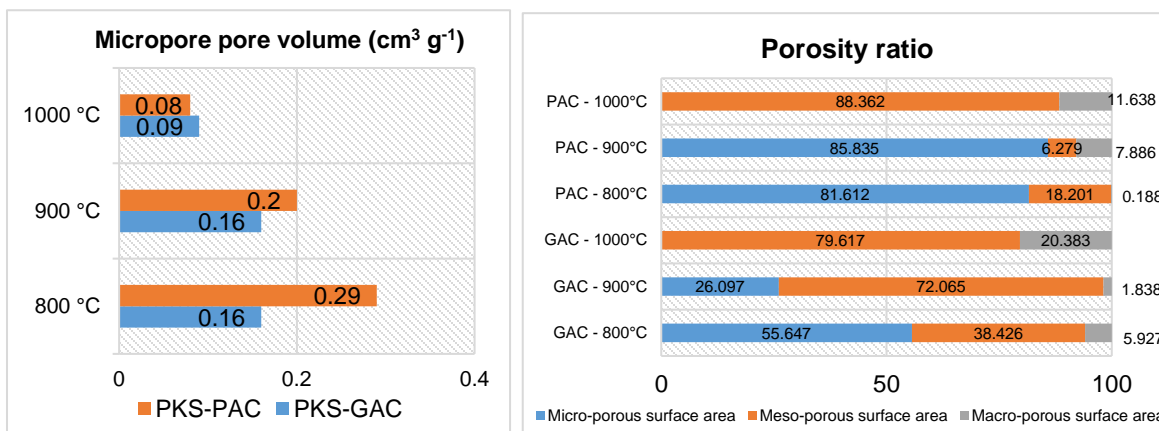
Fig. 2. (**a**) Pore volume and (**b**) porosity ratio for PKS-GAC and PKS-PAC
Note: The particle size range of GAC and PAC are 2 to 5 mm (granular size) and 50 to 85 µm (powdered size), respectively.

N$_2$ Adsorption Isotherm for PKS-GAC and PKS-PAC

Most isotherms have been shown to fit into one of the five IUPAC classification categories. Figure 2 shows that the PKS-PAC prepared at 800 °C in accordance with the type I (a) isotherm. Type I (a) indicates that the samples were microporous materials with primarily narrow micropores (width ~1 nm). Both the AC prepared with 900 and 1000 °C conformed to type IV isotherm. The initial part of the type-IV isotherm for carbon, as shown in Fig. 3, represents micropore filling, and the slope of the plateau at high relative pressure is due to multilayer adsorption on non-microporous surfaces, *i.e*., in mesopores, macropores, and the external surface (Roquerol *et al*. 2013; Wang *et al*. 2013). Figure 3 reveals that activation temperature on different particle sizes had a significant impact on the surface characteristics of AC. Both ACs conformed to type IV (a) and type IV (b) for 900 and 1000 °C, respectively. Type IV (a) isotherms implied that the sample had a mesoporous structure with a high proportion of mesopores and micropores but a low concentration of macropores, whereas type IV (b) isotherms indicated that the AC was given by conical and cylindrical mesopores that were closed at the tapered end. Furthermore, an isotherm profile will be observed for macroporous materials. An apparent increase in adsorption at relatively high pressure ($p/p° > 0.9$) was observed on the sample prepared at 1000 °C. When an isotherm exhibits a sharp increase as $p/p°$ approaches to 1, that indicates the presence of macropores (Teo *et al*. 2017; Lin *et al*. 2019; Duan *et al*. 2021).

According to the authors' previously published work, Sahfani *et al.* (2021), there was a strong significant correlation between the micropores and the specific surface area of the AC derived from PKS. The higher the proportion of micropore, the higher the specific surface area for the AC. In the present study, the results revealed interesting findings on the N$_2$ adsorption isotherm, which correlated with the adsorption result for AC. Adsorption properties, particularly iodine and methylene blue adsorption, are commonly

used parameters as rapid assessment of absorbent quality in AC research. As stated by Chin *et al* (2020) and Benadjemia *et al.* (2011), adsorption of iodine is a measure of micropore content of the activated carbon (0 to 20 Å, or up to 2 nm). Meanwhile, adsorption of methylene blue is mainly used to indicate the mesoporous content of the activated carbon as a minimum pore size of 1.4 to 1.5 nm is required for methylene blue adsorption. The N_2 adsorption isotherm results also support the fact that the activation temperature did influence the surface characteristics of PKS-AC. The pore structure is the primary determinant of adsorptive capacity. The presence of micropores (type I isotherm) was reflected from the high iodine adsorption properties of AC produced at low temperatures, whereas AC produced at high temperatures possesses larger pore sizes/mesopore (type IV isotherm), which can explain the higher methylene blue adsorption properties.
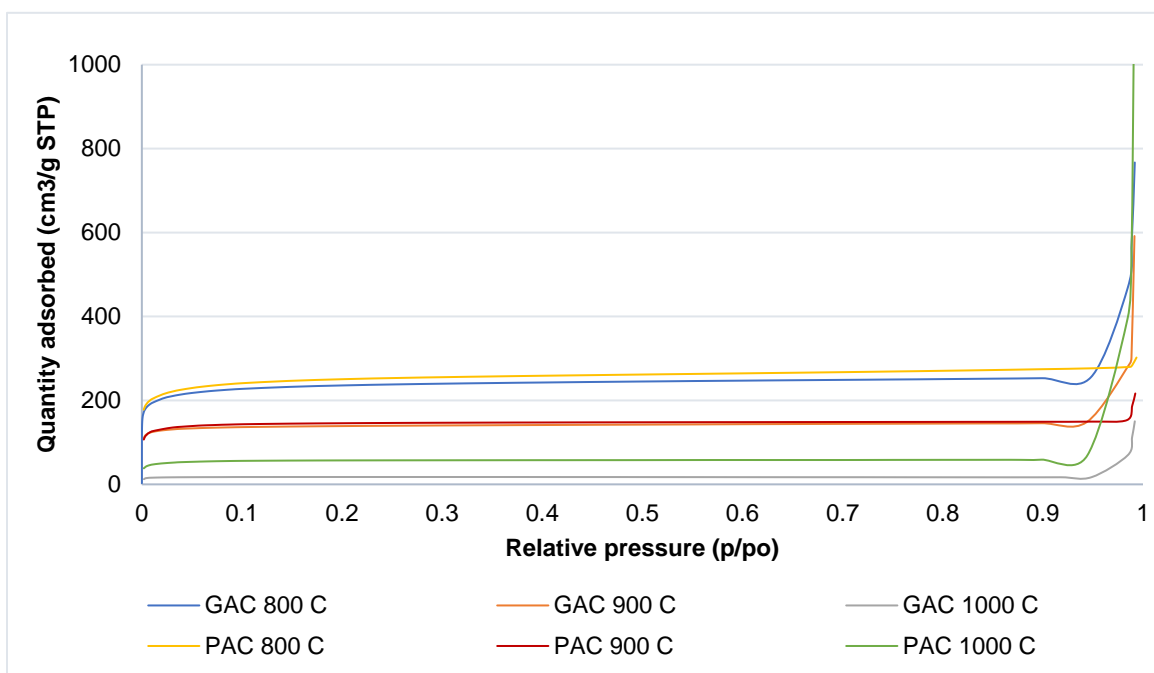
Fig. 3. N_2 adsorption isotherm for PKS-GAC and PKS-PAC
Note: The particle size range of GAC and PAC are 2 to 5 mm (granular size) and 50 to 85 μm (powdered size), respectively.

Surface Morphology of Activated Carbon

SEM was used to examine the surface structure of PKS-GAC and PKS-PAC. The AC prepared using low temperature had higher adsorption performance on iodine and methylene blue than PKS-GAC due to the more developed surface and presence of micropores. A large number of open and orderly pores were formed on PKS-PAC prepared at 800 °C (Fig. 4(b)). In contrast, PKS-GAC prepared at 800 °C had a lower porous structure, based on these observations. The surface morphology of PKS-GAC revealed pores mostly covered with impurities, which would be expected to result in pore blocking and low surface area (Fig. 4(a)). Thus, it is proposed that the presence of impurities on the surface of PKS-GAC resulted in a reduced surface area, implying that the reaction is inhibited. Figures 4(c) and 4(d) show that the surface of PKS-GAC and PKS-PAC began to melt once the temperature reached 900 °C with PKS-GAC showing a more negative impact to the surface structure. As the temperature increased to 1000 °C, PKS-PAC and

PKS-GAC surfaces were completely melted, pores closely connected into a molten and flat surface (Figs. 4 (e) and 4(f)). An increase in activation temperature to 1000 °C leads to the higher carbon breakdown, resulting in the formation of new particles and the enlargement of existing pores (Farma *et al*. 2021). Chin *et al*. (2015) reported that the ash in oil palm biomass was completely melted when exposed to 900 °C, which resulted in molten ash.
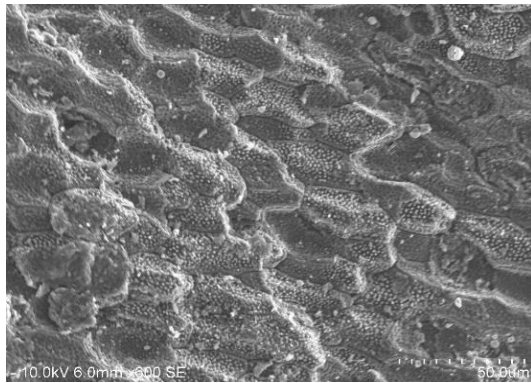
(a) PKS-GAC activated with 800 °C
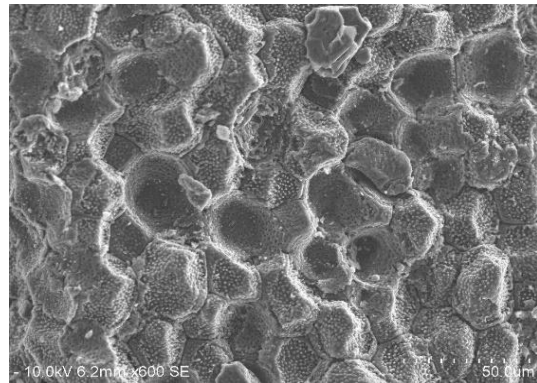
(b) PKS-PAC activated with 800 °C
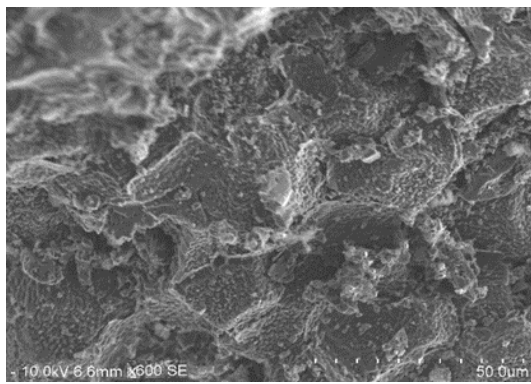
(c) PKS-GAC activated with 900 °C
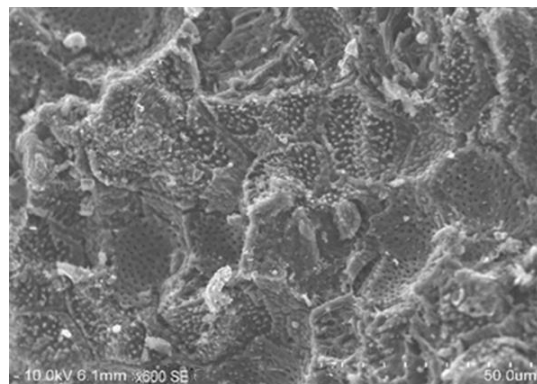
(d) PKS-PAC activated with 900 °C
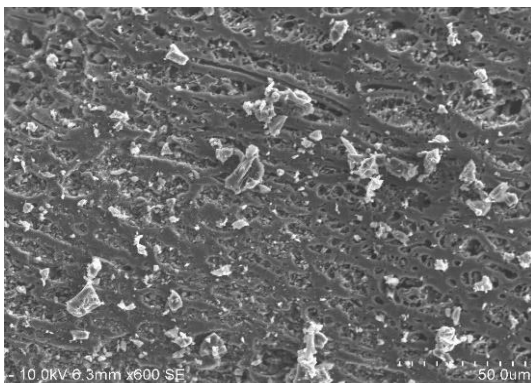
(e) PKS-GAC activated with 1000 °C
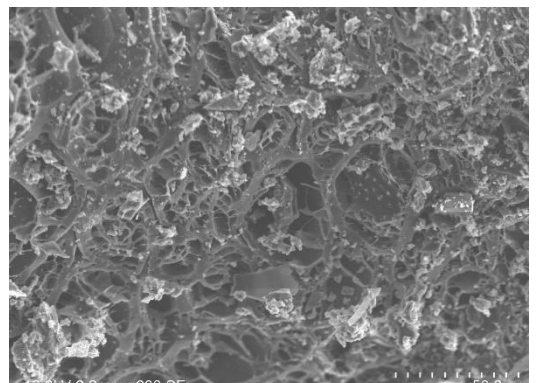
(f) PKS-PAC activated with 1000 °C

Fig. 4. Scanning electron micrographs of PKS-PAC and PKS-GAC
Note: The particle size range of GAC and PAC are 2 to 5 mm (granular size) and 50 to 85 µm (powdered size), respectively.

Surface Chemical Characteristics of Activated Carbon

FTIR is one of the most powerful tools for identifying types of chemical bonds (functional groups) (Islam *et al*. 2022). With an increase in activation temperature, a large amount of oxygen functional groups was eliminated. As shown in Fig. 5 (GAC 800 °C), the 1634 cm^{-1} band indicates the presence of C=O in carboxymethyl cellulose (Tajer *et al*. 2021), while 1930 cm^{-1} bands indicate the presence of C=O stretches in aldehydes, quinones, and carboxyl groups (Guo and Rockstraw 2006; Qu *et al*. 2013). However, neither band were visible after the PKS-GAC sample was subjected to higher temperatures. The oxygen content is significant, and it can contribute to the development of high microporosity during char formation. The removal of oxygen groups will cause significant changes in the networks connecting aliphatic and aromatic bridges. These findings indicate the destruction of crosslinks and the rearrangement of the carbon layer, which resulted in the collapse of pores (Ahmad *et al.* 2013). Furthermore, the FTIR peak positions were shifted towards lower wavelength values, as evident in the PKS-GAC spectra. When the activation temperature was raised from 800 °C to 1000 °C, the peaks shifted to the lower wavelength side from 1730 to 1728 cm^{-1}, 1372 to 1368 cm^{-1}, and 1220 to 1218 cm^{-1}. Accordingly, these three peaks indicate C=O, C-H, and C=O stretching on the carbon surface (Kumari *et al.* 2021). The lower frequencies absorption indicates that the stronger intermolecular interaction (physical crosslinking) between hydrogen in AC and –O–C=O (ester)) led to shorter bonds in the –C=O stretching mode vibration (Jasmi *et al.* 2018). Furthermore, the characteristic peaks of carboxylic acid were located at 1300 to 1200 cm^{-1}. When a peak shifts to smaller wavelengths, it may be explained by bond stresses and deformation vibrations (Shahrashoub and Bakhtiari 2021).
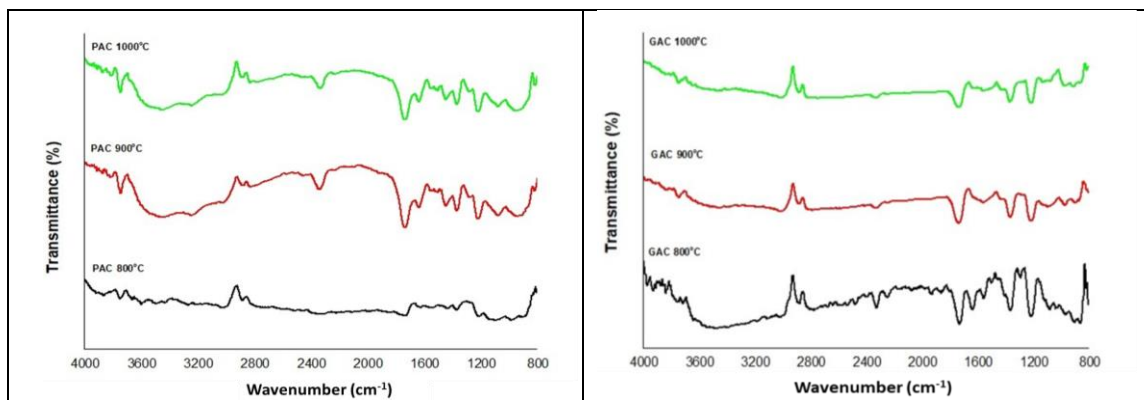
Fig. 5. ATR- FTIR for PKS PAC and PKS-GAC
Note: The particle size range of GAC and PAC are 2 to 5 mm (granular size) and 50 to 85 µm (powdered size), respectively.

The Effect of Particle Size Range on the Characteristics of Activated Carbon

This study showed that particle size range had a significant influence on the pore structure of AC, including specific surface area, pore volume, and average pore width. Compared to the PKS-GAC, the BET surface area of the PKS-PAC was nearly doubled. Based on these high BET values, it was evidenced that PKS-PAC may have a more developed pore network than PKS-GAC. PKS-PAC (Fig. 4(a)) produced rugged surfaces with micropores, indicating that the porous structure was well developed. Additionally, the high micropore surface area and pore volume in PKS-PAC suggest that the surface area increase may be accomplished by the presence of micropores. This study also showed that

the presence of the micropores not only increased the surface area, but it also directly improved the adsorption capability of PKS-PAC. Viscous H_3PO_4 will penetrate more easily into the interior pores of smaller particles than larger particles (Haimour and Emeish 2006). The low iodine adsorption with large particle size (PKS-GAC) was attributed to an increase in external surface area (mesopore and macropore) and a decrease in diffusion path. Figure 2(b) demonstrated that the PKS-PAC was comprised of more than 80% of the micropore surface area, whereas the PKS-GAC had only 55% of the micropore surface area. Thus, PKS-PAC achieved higher iodine adsorption properties than PKS-GAC.

In line with the findings of this study, particle size range is an important factor influencing the methylene blue adsorption properties. This study also demonstrated that activation temperature on different particle size range had an effect on the mesopore domain of AC. Table 1 and Fig. 1(d) illustrate PKS-GAC with high methylene blue capability due to the high amount of mesopore. Even though PKS-GAC provided less iodine adsorption than PKS-PAC owing to its mesopore-rich pore structures, such pore structures have their own specific application. The molecular size of impurities in wastewater treatment, especially dye removal, is complicated, and the presence of mesopores in carbon is advantageous (Lee *et al.* 2019, 2020). Micropore enriched AC is more suitable for the adsorption of small molecular impurities. On the other hand, mesopore-rich pore structures are more suitable for the adsorption of macromolecular impurities (Kang *et al.* 2011; Sun *et al.* 2009). Although the development of micropores smaller than 2 nm can lead to high surface area, they restrict mass transfer and reduce pore accessibility to large adsorbates (Ma *et al.* 2020). In actual water treatment, PKS-GAC with highly developed mesopores could be a better option, which may lead to longer bed life between carbon exchanges, and lower life cycle costs. The high molecular weight organics contained in wastewater may cause micropore blockage and reduce the adsorption capacity of activated, while mesopore (2 nm < diameter < 50 nm) is the main transfer artery for large molecules, higher mesopore may benefit for the adsorbates transfer from liquid solutions to solid adsorbents (Jain *et al.* 2015; Nelson *et al.* 2016; Yu and Luo 2014). Thus, AC should be prepared with a reasonable distribution over the diameter ranges of both micropores and mesopores. Larger particle size allows for fast kinetics and an acceptable pressure drop, while more easily covering a large area (Hansen *et al.* 2010). As a result, the high proportion of mesopore in PKS-GAC could be more reliable than PKS-PAC for the application in wastewater treatment, especially for the textile dye industry.

The low adsorption properties of PKS-GAC can also be explained by the fact that there was a large proportion of ash content in larger particles. As stated by Lee *et al.* (2019), a low ash content is a sign of a high-quality carbon adsorbent. Low ash content in PKS-PAC may lead to superior adsorption of organic compounds from aqueous solution due to the hydrophobicity of the material. High ash content can indeed cause issues to carbon adsorption such as through competitive adsorption, catalysis of adverse reactions, and carbon pore blockage (Deng *et al.* 2003; Serafin *et al.* 2021). In other phrases, as the value of the ash content decreases, the efficiency and adsorptive capacity of the prepared AC increases. Another effect of particle size range in this study is the reduction of mass yield in the AC. Of the mass yield analysed, PKS-PAC experienced a greater mass loss than PKS-GAC. With smaller particle size, the lignin and cellulose in the biomass are more effectively converted due to the higher exposed surface, which leads to higher degrees of thermal reactions (Heidari *et al.* 2018).

As stated previously, the efficiency of AC is improved by increasing surface functional groups. Adsorption capability of AC increased with increasing carbon concentration due to the availability of more surface area and functional groups (Kadirvelu *et al*. 2001). Figures 5 and 6 show that PKS-PAC had more functional groups than PKS-GAC. A broad absorption band was observed in PKS-PAC at 3447 cm^{-1}. This band is assigned to the intramolecular hydroxyl (O-H) stretching mode in the structure (Bora *et al*. 2021). Furthermore, the band 1854 cm^{-1}, which is affiliated with C=O stretching vibration (Tian *et al*. 2020), was present in PKS-PAC but absent from PKS-GAC. The presence of aromatic C=C, a hexagonal form of charcoal, is indicated by absorption at wave number 1500-1400 cm^{-1} (Jeanne Rampe *et al*. 2021). The appearance of the spectrum at wave numbers 1444 cm^{-1} indicates that PKS-PAC samples had formed a C=C bond. Group C=C denotes an increasing carbon content (Maulina and Mentari 2019). Increased efficiency will increase the variety of applications of AC and even provide economic benefits (Arami-Niya *et al*. 2012). This was explained by stating that AC with small particles (PKS-PAC) has superior adsorption properties compared to AC with large particles (PKS-GAC). This research is beneficial and will serve as a foundation for researchers and the AC industry as accurate particle size range will ensure that the most cost-effective AC is chosen to achieve the desired performance objectives.

CONCLUSIONS

1. Particle sizes range was found to have a significant influence on the pore distribution of palm kernel shell activated carbon. Selecting the right type and particle size range is crucial to ensuring an optimal application deployment of porous activated carbon.

2. The presence of micropores, a well-developed pore network, and a high surface functional group, particularly the C=C group, were able to account for the fact that the palm kernel shell – particulate activated carbon (PKS-PAC) outperforming the corresponding granular activated carbon (PKS-GAC).

3. Activation temperature on different particle sizes range has an effect on the mesopore domain of activated carbon. PKS-GAC with a relatively high proportion of mesopore volume is highly demanded for both low mass transfer resistance in pores (fast kinetics) and a high equilibrium adsorption capacity of relatively large dye molecules in the textile industry.

ACKNOWLEDGMENTS

REFERENCES CITED

Ahmad, F., Daud, W. M. A. W., Ahmad, M. A., Radzi, R., and Azmi, A. A. (2013). "The effects of CO_2 activation, on porosity and surface functional groups of cocoa (*Theobroma cacao*) - shell based activated carbon," *Journal of Environmental Chemical Engineering* 1(3), 378-388.

Aktar, M. A., Harun, M. B., and Alam, M. M. (2021). "Green energy and sustainable development," in: *Affordable and Clean Energy. Encyclopedia of the UN Sustainable Development Goals*, W. T. Leal, W. Filho, A. Azul, L. Brandli, and A. Lange Salvia (eds.), Springer, Cham, Switzerland, pp. 719-729. DOI: 10.1007/978-3-319-95864-4_47

Amoatey, P., Izady, A., Al-Maktoumi, A., Chen, M., Al-Harthy, I., Al-Jabri, K., Msagati, T. A. M., Nkambule, T. T. I., and Baawain, M. S. (2021). "A critical review of environmental and public health impacts from the activities of evaporation ponds," *Science of the Total Environment* 796, article 149065. DOI: 10.1016/j.scitotenv.2021.149065

Anonymous. (1992). Japanese Standard Association. Standard testing method of methylene blue number of activated carbon 1470-1991., Japanese industrial standard test method for activated carbon, JIS K.

Arami-Niya, A., Wan Daud, W. M. A., S. Mjalli, F., Abnisa, F., and Shafeeyan, M. S. (2012). "Production of microporous palm shell based activated carbon for methane adsorption: Modeling and optimization using response surface methodology," *Chemical Engineering Research and Design* 90(6), 776-784. DOI: 10.1016/j.cherd.2011.10.001

Aslam, M. A., Ding, W., ur Rehman, S., Hassan, A., Bian, Y., Liu, Q., and Sheng, Z. (2021). "Low cost 3D bio-carbon foams obtained from wheat straw with broadened bandwidth electromagnetic wave absorption performance," *Applied Surface Science* 543, article 148785. DOI: 10.1016/j.apsusc.2020.148785

American Society for Testing and Materials (ASTM D 4607-94). (1994). "Standard test method for determination of iodine number of activated carbon (Reapproved 2006)," ASTM International, West Conshohocken, USA.

Bashir, M. J. K., Jun, Y. Z., Yi, L. J., Abushammala, M. F. M., Amr, S. S. A., and Pratt, L. M. (2020). "Appraisal of student's awareness and practices on waste management and recycling in the Malaysian University's student hostel area," *Journal of Material Cycles and Waste Management* 22(3), 916-927. DOI: 10.1007/s10163-020-00988-6

Bertone, E., Chang, C., Thiel, P., and O'Halloran, K. (2018). "Analysis and modelling of powdered activated carbon dosing for taste and odour removal," *Water Research* 139, 321-328. DOI: 10.1016/j.watres.2018.04.023

Benadjemia, M., Millière, L., Reinert, L., Benderdouche, N., and Duclaux, L. (2011). "Preparation, characterization and methylene blue adsorption of phosphoric acid activated carbons from globe artichoke leaves," *Fuel Processing Technology* 92(6), 1203-1212. DOI: 10.1016/j.fuproc.2011.01.014

Bora, M., Benoy, S. M., Tamuly, J., and Saikia, B. K. (2021). "Ultrasonic-assisted chemical synthesis of activated carbon from low-quality subbituminous coal and its preliminary evaluation towards supercapacitor applications," *Journal of Environmental Chemical Engineering* 9, article 104986. DOI: 10.1016/j.jece.2020.104986

Borghei, S. A., Zare, M. H., Ahmadi, M., Sadeghi, M. H., Marjani, A., Shirazian, S., and Ghadiri, M. (2021). "Synthesis of multi-application activated carbon from oak seeds by KOH activation for methylene blue adsorption and electrochemical supercapacitor electrode," *Arabian Journal of Chemistry* 14, article 102958. DOI: 10.1016/j.arabjc.2020.102958

Chin, K. L., H'ng, P. S., Paridah, M. T., Szymona, K., Maminski, M., Lee, S. H., Lum, W. C., Nurliyana, M. Y., Chow, M. J., and Go, W. Z. (2015). "Reducing ash related operation problems of fast growing timberspecies and oil palm biomass for combustion applications usingleaching techniques," *Energy* 90, 622-630.

Chin, K. L., Lee, C. L., H'ng, P. S., Rashid, U., Paridah, M. T., Khoo, P. S., and Maminski, M. (2020). "Refining micropore capacity of activated carbon derived from coconut shell *via* deashing post- treatment," *BioResources* 15(4), 7749-7769.

Demiral, İ., Samdan, C., and Demiral, H. (2021). "Enrichment of the surface functional groups of activated carbon by modification method," *Surfaces and Interfaces* 22, article 100873. DOI: 10.1016/j.surfin.2020.100873

Deng, S., Bai, R., and Chen, J. P. (2003). "Behaviors and mechanisms of copper adsorption on hydrolyzed polyacrylonitrile fibers," *Journal of Colloid and Interface Science* 260, 265-272. DOI: 10.1016/S0021-9797(02)00243-6

Duan, C., Zou, W., Du, Z., Mi, J., Han, J., and Zhang, C. (2021). "Construction of oxygen-rich carbon foams for rapid carbon dioxide capture," *Materials* 14(1), 1-13. DOI: 10.3390/ma14010173

Farma, R., Putri, A., Taer, E., Awitdrus, A., and Apriwandi, A. (2021). "Synthesis of highly porous activated carbon nanofibers derived from bamboo waste materials for application in supercapacitor," *Journal of Materials Science: Materials in Electronics* 32(6), 7681-7691. DOI: 10.1007/s10854-021-05486-5

Gualtieri, A. F. (2021). "Bridging the gap between toxicity and carcinogenicity of mineral fibres by connecting the fibre crystal-chemical and physical parameters to the key characteristics of cancer," *Current Research in Toxicology* 2, 42-52. DOI: 10.1016/j.crtox.2021.01.005

Guo, Y., and Rockstraw, D. A. (2006). "Physical and chemical properties of carbons synthesized from xylan, cellulose, and kraft lignin by H_3PO_4 activation," *Carbon* 44(8), 1464-1475. DOI: 10.1016/j.carbon.2005.12.002

Haimour, N. M., and Emeish, S. (2006). "Utilization of date stones for production of activated carbon using phosphoric acid," *Waste Management* 26, 651-660. DOI: 10.1016/j.wasman.2005.08.004

Hansen, M. C., Børresen, M. H., Schlabach, M., and Cornelissen, G. (2010). "Sorption of perfluorinated compounds from contaminated water to activated carbon," *Journal of Soils and Sediments* 10(2), 179-185. DOI: 10.1007/s11368-009-0172-z

Hassan, N., Abdullah, R., Khadiran, T., Elham, P., and Vejan, P. (2021). "Biochar derived from oil palm trunk as a potential precursor in the production of high-performance activated carbon," *Biomass Conversion and Biorefinery* 2021, 1-17. DOI: 10.1007/s13399-021-01797-z

Heidari, M., Salaudeen, S., Dutta, A., and Acharya, B. (2018). "Effects of process water recycling and particle sizes on hydrothermal carbonization of biomass," *Energy and Fuels* 32(11), 11576-11586.

Hidayu, A. R., and Muda, N. (2016). "Preparation and characterization of Impregnated activated carbon from palm kernel shell and coconut shell for CO_2 Capture," *4th International Conference on Process Engineering and Advanced Materials* 148, 106–113. DOI: 10.1016/j.proeng.2016.06.463

Islam, M. N., Khatton, A., Sarker, A., Sikder, H. A., and Chowdhury, A. M. S. (2022). "Preparation and characterization of activated carbon from jute stick by chemical activation: Comparison of different activating agents," *Saudi Journal of Engineering and Technology* 7(2), 112-117. DOI: 10.36348/sjet.2022.v07i02.008

Jain, A., Balasubramanian, R., and Srinivasan, M. P. (2015). "Tuning hydrochar properties for enhanced mesopore development in activated carbon by hydrothermal carbonization," *Microporous and Mesoporous Materials* 203, 178-185. DOI: 10.1016/j.micromeso.2014.10.036

Jasmi, F., Azeman, N. H., Bakar, A. A. A., Zan, M. S. D., Haji Badri, K., and Su'ait, M. S. (2018). Ionic conductive polyurethane-graphene nanocomposite for performance enhancement of optical fiber bragg grating temperature sensor. *IEEE Access*, 6, 47355–47363.

Japanese Industrial Standards (JIS (1992). "Japanese industrial standard testing method of methylene blue number of activated carbon," 1470-1991.

Jeanne Rampe, M., Santoso, I. R. S., Rampe, H. L., Tiwow, V. A., and Apita, A. (2021). "Infrared spectra patterns of coconut shell charcoal as result of pyrolysis and acid activation origin of Sulawesi, Indonesia," in: *E3S Web of Conferences*, 08008. DOI: 10.1051/e3sconf/202132808008

Joseph, S., Peacocke, C., Lehmann, J., and Munroe, P. (2009). *Biochar for Environmental Management: Science and Technology*, J. Lehmann and S. Joseph, (eds.), Earthscan, London.

Kadirvelu, K., Thamaraiselvi, K., and Namasivayam, C. (2001). "Adsorption of nickel(II) from aqueous solution onto activated carbon prepared from coirpith," *Separation and Purification Technology* 24, 497-505. DOI: 10.1016/S1383-5866(01)00149-6

Kang, S., Jiang, J.-C., and Cui, D.-D. (2011). "Preparation of activated carbon with highly developed mesoporous structure from Camellia oleifera shell through water vapor gasification and phosphoric acid modification," *Biomass and Bioenergy* 35(8), 3643-3647. DOI: 10.1016/j.biombioe.2011.05.007

Lee, C. L., H'ng, P. S., Paridah, M. T., Chin, K. L., Khoo, P. S., Nazrin, R. A. R., Asyikin, S. N., and Mariusz, M. (2017). "Effect of reaction time and temperature on the properties of carbon black made from palm kernel and coconut shell," *Asian Journal of Scientific Research*, 10(1), 24-33. DOI: 10.3923/ajsr.2017.Research

Lee, C. L., H'ng, P. S., Chin, K. L., Paridah, M. T., Rashid, U., Maminski, M., Go, W. Z., Nazrin, R. A. R., Rosli, S. N. A., and Khoo, P. S. (2018). "Production of bioadsorbent from phosphoric acid pretreated palm kernel shell and coconut shell by two-stage continuous physical activation *via* N_2 and air," *Royal Society Open Science* 5(12), article 180775. DOI: 10.1098/rsos.180775

Lee, C. L., H'ng, P. S., Chin, K. L., Paridah, M. T., Rashid, U., and Go, W. Z. (2019). "Characterization of bioadsorbent produced using incorporated treatment of chemical and carbonization procedures," *Royal Society Open Science* 6(9), article 190667. DOI: 10.1098/rsos.190667

Lee, C. L., H, P. S., Chin, K. L., Rashid, U., Maminski, M., and Paridah, T. (2020). "Effect of pretreatment conditions on the chemical- structural characteristics of coconut and palm kernel shell: A potentially valuable precursor for eco-efficient activated carbon production," *Environmental Technology & Innovation* 21, article 101309. DOI: 10.1016/j.eti.2020.101309

Li, X. R., Jiang, Y. H., Wang, P. Z., Mo, Y., Lai, W. De, Li, Z. J., Yu, R. J., Du, Y. T., Zhang, X. R., and Chen, Y. (2020). "Effect of the oxygen functional groups of activated carbon on its electrochemical performance for supercapacitors," *Xinxing Tan Cailiao/New Carbon Materials* 35(3), 232-243. DOI: 10.1016/S1872-5805(20)60487-5

Lin, Y., Chen, Z., Yu, C., and Zhong, W. (2019). "Heteroatom-doped sheet-like and hierarchical porous carbon based on natural biomass small molecule peach gum for high-performance supercapacitors," *ACS Sustainable Chemistry and Engineering* 7(3), 3389-3403. DOI: 10.1021/acssuschemeng.8b05593

Ma, R., Ma, Y., Gao, Y., and Cao, J. (2020). "Preparation of micro-mesoporous carbon from seawater-impregnated sawdust by low temperature one-step CO_2 activation for adsorption of oxytetracycline," *SN Applied Sciences* 2(2), 1-15. DOI: 10.1007/s42452-020-1940-z

Maulina, S., and Mentari, V. A. (2019). "Comparison of functional group and morphological surface of activated carbon from oil palm fronds using phosphoric acid (H_3PO_4) and nitric acid (HNO_3) as an activator," *IOP Conference Series: Materials Science and Engineering* 505, article 012023. DOI: 10.1088/1757-899X/505/1/012023

Mendes, F. M. T., Marques, A. C. C., Mendonça, D. L., Oliveira, M. S., Moutta, R. O., and Ferreira-Leitão, V. S. (2015). "High surface area activated carbon from sugar cane straw," *Waste and Biomass Valorization* 6, 433-440. DOI: 10.1007/s12649-015-9356-5

Nelson, K. M., Mahurin, S. M., Mayes, R. T., Williamson, B., Teague, C. M., Binder, A. J., Baggetto, L., Veith, G. M., and Dai, S. (2016). "Preparation and CO_2 adsorption properties of soft-templated mesoporous carbons derived from chestnut tannin precursors," *Microporous and Mesoporous Materials* 222, 94-103. DOI: 10.1016/j.micromeso.2015.09.050

Norrrahim, M. N. F., Farid, M. A. A., Lawal, A. A., Tengku Arisyah, T. Y.-A., Samsudin, M. H., and Zulkifli, A. A. (2022). "Emerging technologies for value-added use of oil palm biomass," *Environmental Science: Advances*. DOI: 10.1039/d2va00029f

Oguntoke, O., Emoruwa, F. O., and Taiwo, M. A. (2019). "Assessment of air pollution and health hazard associated with sawmill and municipal waste burning in Abeokuta Metropolis, Nigeria," *Environmental Science and Pollution Research* 26(32), 32708-32722. DOI: 10.1007/s11356-019-04310-2

Olajide, M. J. (2019). "Remediation of Cr (VI) from contaminated water by activated carbon entrapped in calcium alginate beads," *Afribary*, 21 May 2021, https://afribary.com/works/remediation-of-cr-vi-from-contaminated-water-by-actvated-carbon-entrapped-in-calcium-alginate-beads.

Philibert, M., Zacchi, C. M., Pottier, C., Sacareau, D., and Baudin, I. (2020). "Mechanical resistance of granular activated carbon media in drinking water treatment," *Water and Environment Journal*, 34, 381–389. DOI: 10.1111/wej.12535

Qu, G., Liang, D., Qu, D., Huang, Y., Liu, T., Mao, H., Ji, P., and Huang, D. (2013). "Simultaneous removal of cadmium ions and phenol from water solution by pulsed corona discharge plasma combined with activated carbon," *Chemical Engineering Journal* 228, 28-35. DOI: 10.1016/j.cej.2013.04.114

Rashidi, N. A., and Yusup, S. (2021). "Co-valorization of delayed petroleum coke – palm kernel shell for activated carbon production," *Journal of Hazardous Materials* 403, article 123876. DOI: 10.1016/j.jhazmat.2020.123876

Roquerol, F., Rouquerol, J., and Sing, K. (2013). *Adsorption by Powders and Solids: Principles, Methodology, and Applications*, Academic Press, Elsevier.

Sahfani, M. N. H., Lee, C. L., Chin, K. L., H, P. S., Khoo, P. S., and Rashid, U. (2021). "Fabrication of highly microporous structure activated carbon *via* surface modification with sodium hydroxide," *Polymers* 13(22), 3954.

Samal, D. P. (2014). "Characterization of activated carbon and study of adsorption of methylene blue dye using activated carbon," National Institute of Technology, Rourkela.

Sarwer, A., Hamed, S. M., Osman, A. I., Jamil, F., Al-muhtaseb, A. H., Alhajeri, N. S., and Rooney, D. W. (2022). "Algal biomass valorization for biofuel production and carbon sequestration : a review," *Environmental Chemistry Letters* 20, 2791-2851. DOI: 10.1007/s10311-022-01458-1

Serafin, J., Ouzzine, M., Cruz, O. F., Sreńscek-Nazzal, J., Campello Gómez, I., Azar, F. Z., Rey Mafull, C. A., Hotza, D., and Rambo, C. R. (2021). "Conversion of fruit waste-derived biomass to highly microporous activated carbon for enhanced CO_2 capture," *Waste Management* 136, 273-282. DOI: 10.1016/j.wasman.2021.10.025

Shahrashoub, M., and Bakhtiari, S. (2021). "The efficiency of activated carbon/magnetite nanoparticles composites in copper removal: Industrial waste recovery, green synthesis, characterization, and adsorption-desorption studies," *Microporous and Mesoporous Materials* 311, article 110692. DOI: 10.1016/j.micromeso.2020.110692

Sun, K., Jiang, J., and Lu, X. (2009). "Preparation of activated carbon from *Xanthoceras sorbifolia* Bunge hull and its application for decolorization and deodorization of glycerin," *Chemistry and Industry of Forest Products* 29, 77-81.

Tajer, M., Anbia, M., and Salehi, S. (2021). "Fabrication of polyacrylonitrile hybrid nanofiber scaffold containing activated carbon by electrospinning process as nanofilter media for SO_2, CO_2, and CH_4 adsorption," *Environmental Progress and Sustainable Energy* 40(1), 13498. DOI: 10.1002/ep.13498

"Technical Association of the Pulp, & Paper Industry." (1992).

TAPPI T211 OM-85. (1991). "Ash in wood and pulp," TAPPI Press, Atlanta, GA.

Teo, H. W. B., Chakraborty, A., Kitagawa, Y., and Kayal, S. (2017). "Experimental study of isotherms and kinetics for adsorption of water on aluminium fumarate," *International Journal of Heat and Mass Transfer* 114, 621-627. DOI: 10.1016/j.ijheatmasstransfer.2017.06.086

Tian, D., Xu, Z., Zhang, D., Zhou, Y., and Sun, Z. (2020). "Multifaceted roles of $FeCl_2$ on pore formation of polyester fabric wastes-based activated carbon," *Colloids and Surfaces A: Physicochemical and Engineering Aspects* 598, article 124756. DOI: 10.1016/j.colsurfa.2020.124756

Vu, T. P., Vogel, A., Kern, F., Platz, S., Menzel, U., and Gadow, R. (2014). "Characteristics of an electrocoagulation-electroflotation process in separating powdered activated carbon from urban wastewater effluent," *Separation and Purification Technology* 134, 196–203. DOI: 10.1016/j.seppur.2014.07.038

Wang, X., Li, D., Li, W., Peng, J., Xia, H., Zhang, L., Guo, S., and Chen, G. (2013). "Optimization of mesoporous activated carbon from coconut shells by chemical activation with phosphoric acid," *BioResources* 8(4), 6184-6195.

Yu, L., and Luo, Y. M. (2014). "The adsorption mechanism of anionic and cationic dyes by Jerusalem artichoke stalk-based mesoporous activated carbon," *Journal of Environmental Chemical Engineering* 2(1), 220-229. DOI: 10.1016/j.jece.2013.12.016

Zhang, G., Lei, B., Chen, S., Xie, H., and Zhou, G. (2021). "Activated carbon adsorbents with micro-mesoporous structure derived from waste biomass by stepwise activation for toluene removal from air," *Journal of Environmental Chemical Engineering* 9, 105387. DOI: 10.1016/j.jece.2021.105387